JOURNAL OF VIROLOGY, Aug. 1984, p. 306–314
0022-538X/84/080306-09$02.00/0

Vol. 51, No. 2

Heteroduplex Analysis of Molecular Clones of the Pathogenic Friend Virus Complex: Friend Murine Leukemia Virus, Friend Mink Cell Focus-Forming Virus, and the Polycythemia- and Anemia-Inducing Strains of Friend Spleen Focus-Forming Virus

MATTHEW A. GONDA,[1]* JOSEPH KAMINCHICK,[2] ALLEN OLIFF,[3] JOHN MENKE,[2] KUNIO NAGASHIMA,[1] AND EDWARD M. SCOLNICK[4]

Electron Microscopy Laboratory, Program Resources, Inc., National Cancer Institute-Frederick Cancer Research Facility, Frederick, Maryland 21701[1]; Laboratory of Tumor Virus Genetics, National Cancer Institute, Bethesda, Maryland 20205[2]; DeWitt Wallace Research Laboratory, Memorial Sloan-Kettering Cancer Center, New York, New York 10021[3]; and Merck Sharp & Dohme Research Laboratories, West Point, Pennsylvania 19486[4]

Received 19 January 1984/Accepted 10 May 1984

The pathogenic Friend virus complex is of considerable interest in that, although members of this group are genetically related, they differ markedly in biochemical and biological properties. Heteroduplex mapping of molecular clones of the Friend virus complex, which includes the replication-competent ecotropic Friend murine leukemia virus (F-MuLV) and mink cell focus-forming virus (F-MCF) and replication-defective polycythemia- and anemia-inducing strains of spleen focus-forming virus ($SFFV_p$ and $SFFV_a$, respectively), was employed to provide insight into the molecular basis of their relationships. In heteroduplexes of F-MuLV × F-MCF, a major substitution of 0.89 kilobases in the *env* gene of F-MCF was discerned. Heteroduplexes of $SFFV_p$ × F-MuLV or F-MCF and $SFFV_a$ × F-MuLV or F-MCF showed several major deletions in the *pol* gene region and a single major deletion in the 3′ half of the *env* gene region of $SFFV_p$ and $SFFV_a$. A major substitution of 0.89 kilobases was mapped to the 5′ end of the *env* deletion of $SFFV_p$ and $SFFV_a$ in heteroduplexes with F-MuLV, similar to that seen in F-MuLV × F-MCF heteroduplexes. In contrast, this *env* gene region was totally homologous in F-MCF × $SFFV_p$ or $SFFV_a$ and $SFFV_p$ × $SFFV_a$ heteroduplexes. Our results suggest that (i) both $SFFV_p$ and $SFFV_a$ lack part of the *env* gene at its 3′ end, corresponding to the p15(E) coding region, (ii) major deletions occur in the *pol* and *env* genes which account for the replication defectiveness of $SFFV_p$ and $SFFV_a$, (iii) minor substitutions occur in the *gag* gene region of $SFFV_a$ that are not present in $SFFV_p$, F-MuLV, or F-MCF, (iv) a major substitution exists in the gp70 region of the *env* gene between F-MuLV and F-MCF that probably accounts for the differences in their host range specificities, (v) this substitution in F-MCF is identical to the gp70 part of the gp52 coding region of $SFFV_p$ and $SFFV_a$, and (vi) heteroduplexes to F-MCF show unambiguously that no additional large substitutions are present in $SFFV_p$ or $SFFV_a$ that could account for differences in their leukemogenicity.

The original isolate of Friend virus described in 1957 caused acute erythroblastosis associated with anemia (13). Passage of this Friend virus stock in several laboratories has resulted in the identification of several pathogenic strains that differ in their biological and biochemical properties (for a review, see reference 44). For example, Axelrad and Steeves (2) and Mirand et al. (24) described strains of Friend virus that caused polycythemia in susceptible mice, rather than anemia as originally described (13). Although all of these "strains" produce rapid erythroid proliferation, erythroleukemia, splenomegaly, and splenic foci, they can be distinguished by diagnosis of the terminal stages of their disease as being accompanied by polycythemia or anemia (2, 13, 24, 37, 44).

The polycythemia and anemia strains of the Friend virus complex are each composed of at least two distinct viral components: (i) a replication-competent, ecotropic helper type C virus (F-MuLV) (23, 26, 38, 43, 45, 46) and (ii) a replication-defective, spleen focus-forming virus (SFFV) (18, 21, 42, 43). Alone, F-MuLV causes a relatively rapid erythroleukemia in susceptible newborn mice; however, F-MuLV does not induce this disease syndrome in adult mice. Uncloned polycythemia and anemia strains have the ability to cause erythroleukemia in both newborn and adult mice in addition to causing the characteristic splenic foci. Furthermore, pseudotypes of SFFV with thymic or lymphatic leukemia viruses also cause their characteristic erythroproliferative disease with associated splenic foci, suggesting that the SFFV component of polycythemia and anemia strains ($SFFV_p$ and $SFFV_a$, respectively) are solely responsible for the production of polycythemia and anemia (44).

$SFFV_p$ and $SFFV_a$ infected cells synthesize a viral glycoprotein with a molecular weight of approximately 52,000 (gp52), which is not shed from cells or incorporated into virions and which shares antigenic determinants with the major 70,000-molecular-weight glycosylated envelope protein (gp70) of Friend mink cell focus-forming virus (F-MCF) not present on F-MuLV gp70 (31, 32, 35, 43, 44, 47). The association of gp52 with Friend erythroleukemia suggests that it is essential for the maintenance of the SFFV-induced disease. Using a two-stage cotransfection assay with subgenomic fragments derived from $SFFV_p$ and $SFFV_a$, Linemeyer et al. (22) and Kaminchick et al. (18) have confirmed this hypothesis and biologically traced the pathogenicity of each strain to a 3′ subgenomic fragment coding for the gp52s. However, the molecular basis for differences in the pathogenicity of $SFFV_p$ and $SFFV_a$ remained to be determined.

The molecular cloning of each of the individual compo-

* Corresponding author.

nents of the Friend virus complex (F-MuLV, F-MCF, SFFV$_p$, and SFFV$_a$) now makes such analyses possible (18, 21, 26, 27). We employed these molecular clones in detailed heteroduplex mapping studies to define sequence homologies and differences between F-MuLV, F-MCF, SFFV$_p$, and SFFV$_a$ strains and to derive molecular information about the origin and distinctive biological properties responsible for the erythroproliferative diseases induced by the members of the pathogenic Friend virus complex, focusing in particular on the relationship of SFFV$_p$ to SFFV$_a$. Although heteroduplex mapping demonstrated homology to and conservation of F-MCF *env* sequences in SFFV$_p$ and SFFV$_a$ in the region believed to be responsible for the SFFV-induced disease, no clear demonstration of molecular differences between SFFV$_p$ and SFFV$_a$ was obtained that could account for their individual and unique pathogenic properties.

(This work was presented in part at the UCLA Symposium on Tumor Viruses and Differentiation, Squaw Valley, Calif., 21 to 28 March 1982.)

MATERIALS AND METHODS

Cloned viral DNAs. The strategies for cloning and characterizing the F-MuLV (26), F-MCF (27), SFFV$_p$ (21), and SFFV$_a$ (18) viral genomes were previously described, as were the restriction enzyme maps (18, 21, 26, 27). The viral inserts were freed from their cloning vectors by restriction enzyme digestion and preparative gel electrophoresis in low-melting-temperature agarose (Bethesda Research Laboratories, Bethesda, Md.) according to the manufacturer's specifications. The DNA was further purified by phenol extraction (2×), ethanol precipitation, and pelleting. DNA for heteroduplexing was dissolved in a solution of 10 mM Tris-hydrochloride and 1 mM EDTA (pH 7.2) and brought to a final concentration of 0.1 mg/ml.

Heteroduplexing and electron microscopy. Heteroduplexes were prepared by the method of Davis et al. (10). Briefly, a mixture of linear DNA (0.1 μg of each) was denatured in 0.1 N NaOH for 10 min at 37°C. The solution was neutralized by the addition of 0.2 volume of 1 M Tris-hydrochloride (pH 7.0). Deionized formamide was added to a final concentration of 50%, and renaturation at room temperature was permitted for 15 to 30 min. The heteroduplexes were immediately mounted for electron microscopy by the basic protein film technique (10). Hyperphases typically contained 100 mM TES [*N*-tris(hydroxymethyl)methyl-2-aminoethanesulfonic acid] (pH 8.5), 10 mM EDTA, cytochrome *c* at a concentration of 30 to 50 μg/ml, and the duplexed DNA (49). To obtain a differential in the effective temperature at which DNA was mounted for electron microscopy, the concentration of formamide in the hyperphase was varied from 40 to 70% (9). The salt concentration and pH were kept constant. Heteroduplexes were rotary shadowed with platinum-palladium and were examined and photographed in a Hitachi HU-12A electron microscope at 25 kV. Contour lengths were measured from actual micrographs with a digital length calculator (Numonics Corp., Lansdale, Pa.). The sizes of cloned DNAs were determined comparatively in separate gel electrophoresis experiments.

RESULTS

Restriction enzyme maps: comparison of F-MuLV, F-MCF, SFFV$_p$, and SFFV$_a$. The restriction enzyme maps shown in Fig. 1 were compiled from references 18, 21, 26, and 27. All genomes were cloned in a permuted fashion with respect to their viral RNAs from circular proviral DNA obtained from Hirt extractions of newly infected cells. The F-MuLV genome was cloned at an *Eco*RI site in the *gag* gene region of the genome. This clone is 8.3 kilobase pairs (kbp) in length and contains a single long terminal repeat (LTR) (26). The F-MCF genome was cloned at an *Sph*I site at or near the 3′ terminus of the *pol* gene. This clone is 8.2 kbp in length and contains a single copy of the LTR (27). The SFFV$_p$ genome was cloned at a unique *Hin*dIII site, also at or near the 3′ terminus of the *pol* gene. This clone is 5.7 kbp in length and contains a single copy of the LTR (21). The SFFV$_a$ genome was cloned at a unique *Cla*I site near the 3′ terminus of the *env* gene. This clone is 5.3 kbp long and contains two copies of the LTR (18). The cloning strategies were fortuitous and permitted a clear and easy identification of complete heteroduplexes since overlapping arms of each genome of the recombinant molecule generated a circular heteroduplex (49). Only complete circular heteroduplexes were utilized in these studies. It was also fortunate that one of the clones, SFFV$_a$, had two copies of the LTR; thus, in heteroduplexes with other clones containing a single copy of the LTR, a 500-base pair substitution would be present that could be easily identified and definitely assigned to the SFFV$_a$ genome. We used this feature to our advantage as it provided a method of determining the 5′ and 3′ junctions of the permuted duplexed recombinants. As can be seen by comparing the compilation of the unpermuted, colinear restriction enzyme maps of these viruses (Fig. 1), F-MuLV and F-MCF appeared to be very closely related, sharing common enzyme sites throughout their *gag*, *pol*, and LTR regions; however, they differed in multiple restriction sites in the *env* gene. With the

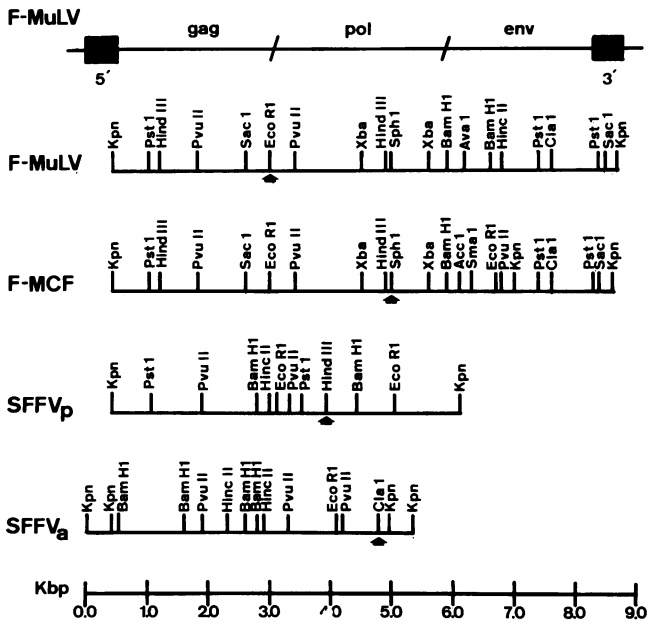

FIG. 1. Restriction endonuclease maps of F-MuLV, F-MCF, SFFV$_p$, and SFFV$_a$ molecular clones schematically drawn in colinear form (information derived from references 18, 21, 26, and 27). An integrated F-MuLV genome (top) is schematically drawn with two LTRs (black boxes) and labeled to show the relative positions of the *gag*, *pol*, and *env* genes. All cloned genomes have been unpermuted and aligned at a single *Kpn* site in the LTR, a portion of which now resides at the 5′ and 3′ ends of the linearized genomes (with the exception of SFFV$_a$, which contains a complete permuted LTR at each end). The black arrows beneath the restriction maps indicate the particular site at which each of the genomes was cloned into pBR322.

exception of this similarity, any relationship among the maps of these viruses is more obscure.

Heteroduplex mapping. (i) Analysis of F-MuLV and F-MCF genomes. Despite the lack of similarity in the restriction enzyme maps among the members of this virus complex (with the exceptions noted) compared in Fig. 1, nucleic acid hybridization data have shown that SFFVs are recombinant viruses composed of sequences in F-MuLV and unique SFFV sequences related to F-MCF (40, 41, 44, 46). Furthermore, F-MuLV and F-MCF are replication-competent viruses of full genomic length, whereas the smaller SFFVs are replication defective; their smaller sizes suggest that major deletions have occurred. To demonstrate and localize the molecular basis for the differences and similarities that exist between members of this family, heteroduplexes were constructed between F-MuLV and F-MCF and spread from high (60% formamide) and low (40% formamide) stringency hyperphases. A heteroduplex of F-MuLV and F-MCF is shown in Fig. 2A to F. In the heteroduplex figures (see Fig. 2 to 7),

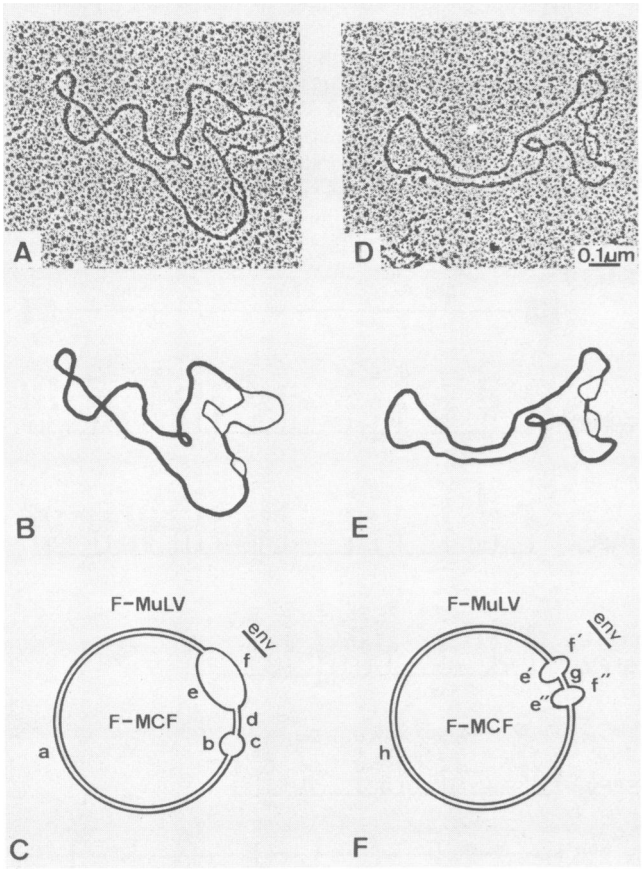

FIG. 2. Heteroduplex analysis of the relationship between F-MuLV and F-MCF clones. Heteroduplexes were mounted for electron microscopy from 60% (A to C) and 40% (D to F) formamide. (A and D) Actual heteroduplexes; (B and E) interpretive drawings; (C and F) schematic representations. The dimensions given in C and F are based on measurements of more than 20 molecules. Contour lengths (in kb) for C were as follows: a, 6.73 ± 0.28; b, 0.21 ± 0.05; c, 0.22 ± 0.04; d, 0.30 ± 0.05; e, 0.89 ± 0.09; f, 1.05 ± 0.12. Dimensions for F-MuLV are a, c, d, and f; those for F-MCF are a, b, d, and e. Contour lengths (in kb) for F were as follows: h, 7.43 ± 0.29; e′, 0.36 ± 0.05; f′, 0.40 ± 0.05; g, 0.12 ± 0.04; e″, 0.23 ± 0.04, and f″, 0.34 ± 0.06. Dimensions for F-MuLV are h, f′, g, and f″; dimensions for F-MCF are h, e′, g, and e″.

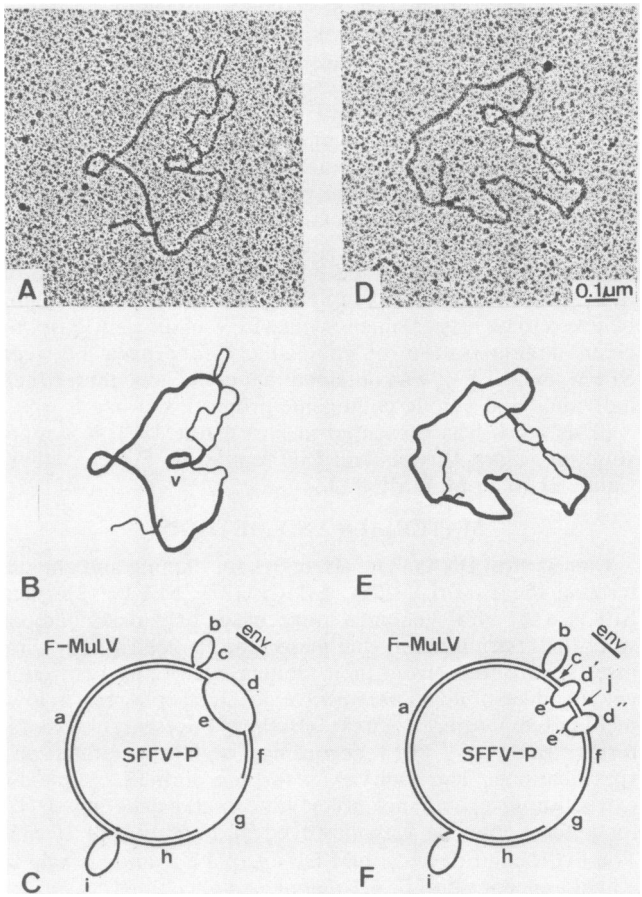

FIG. 3. Heteroduplex analysis of the relationship between F-MuLV and $SFFV_p$ clones. Heteroduplexes were mounted for electron microscopy from 60% (A to C) and 40% (D to F) formamide. (A and D) Actual heteroduplexes; (B and E) interpretive drawings; (C and F) schematic representations. The dimensions given in C and F are based on measurements of over 20 molecules. Contour lengths (in kb) for C were as follows: a, 3.01 ± 0.18; b, 0.69 ± 0.09; c, 0.15 ± 0.03; d, 1.02 ± 0.14; e, 0.89 ± 0.12; f, 0.64 ± 0.06; g, 0.95 ± 0.15; h, 1.10 ± 0.17; and i, 0.73 ± 0.08. Dimensions for F-MuLV are a, b, c, d, f, g, h, and i; dimensions for $SFFV_p$ are a, c, e, f, and h. Contour lengths (in kb) for F were as follows: a, 2.92 ± 0.13; b, 0.69 ± 0.08; c, 0.24 ± 0.06; d′, 0.35 ± 0.05; e′, 0.33 ± 0.05; j, 0.15 ± 0.04; d″, 0.36 ± 0.06; e″, 0.24 ± 0.05; f, 0.75 ± 0.08; g. 0.98 ± 0.09; h, 1.16 ± 0.08; and i, 0.78 ± 0.08. Dimensions for F-MuLV are a, b, c, d′, j, d″, f, g, h, and i; dimensions for $SFFV_p$ are a, c, e′, j, e″, f, and h.

all actual heteroduplexes, interpretive drawings, and schematic representations are oriented such that the LTR region is at the top (12 o'clock) of each circular heteroduplex. This orientation allowed *gag*, *pol*, and *env* gene regions to be located by counterclockwise movement from this point. In spreads from 60% formamide (Fig. 2A to C), two substitutions were seen; the exact location within the genome could not be immediatley determined. In a previous study, in which heteroduplexes between cloned AKR ecotropic and MCF viruses were performed and spread under similar conditions, a single unequal substitution was localized in the *env* region that occurred in two forms (29). The majority of these heteroduplexes appeared to be like ours (Fig. 2A to C). However, in the study by Rapp et al. (29), when the stringency was lowered, a second form appeared that had a small region of homology within the middle of the substitu-

tion (0.13 kilobases [kb]). When we reduced the spreading conditions to 40% formamide, the larger of the two substitutions (Fig. 2A to C, features e and f) annealed in the middle and appeared to be like those described above for cloned AKR ecotropic and MCF viruses (Fig. 2D to F, features e′, f′, g, e″, and f″). The smaller substitution (Fig. 2A to C, features c and b) appeared to reside in the 3′ terminus of the *pol* gene, as it was not present under the milder conditions here and as substantiated in the heteroduplexes described below; thus, we consider it to be of minor importance.

To confirm that the larger substitution was indeed in the *env* gene region, heteroduplexes were performed between the complete F-MCF genome and a subgenomic fragment (*Hin*dIII to *Xba*) that encompasses all of the *env* gene through the LTR and the NH_2-terminal coding portion of the *gag* gene of F-MuLV (Fig. 1). This fragment contains the sequences responsible for F-MuLV–induced erythroleukemia (28). Again, heteroduplexes were mounted for electron microscopy from 60 and 40% formamide. A similar topographical distribution of features was present, with the exception of the minor substitution seen in Fig. 2A to C (features b and c), demonstrating that the major substitution of 0.89 kb was indeed derived from the *env* region (data not shown). Further confirmation of this assignment was derived from heteroduplexes of F-MuLV to SFFV$_p$ and SFFV$_a$, described below.

(ii) Analysis of F-MuLV and SFFV$_p$ genomes. A heteroduplex analysis of F-MuLV and SFFV$_p$ cloned genomes is shown in Fig. 3A to F. Under strong denaturing conditions (Fig. 3A to C), a single large substitution (Fig. 3C, segments d and e) and three deletions (Fig. 3C, segments b, g, and i) were apparent. The substitution was similar to that seen in the *env* gene region between F-MuLV and F-MCF genomes (Fig. 2) and, in spreads from lower stringencies, demonstrated the small region of homology in the middle of the substitution (Fig. 3D to F, segment j). The smaller of the deletions (Fig. 3C and F, segment b) appeared to be at the 3′ end of the *env* region. This deletion maps in the p15(E) region of the *env* sequences. The protein studies of Schultz et al. (36) demonstrated the absence of p15(E) antigen in SFFV nonproducer cells; however, it was not clearly established whether the lack of p15(E) determinants represented a substitution of only a few amino acid residues involved in forming p15(E) antigenic sites or whether there was a deletion of p15(E) sequences. Recent nucleotide sequencing data (7, 48) have clearly established that most p15(E) sequences are deleted as shown here in the heteroduplexes, with the exception of the most carboxy-terminal sequences, which have two unique insertions that could account for lack of immunological detection with anti-p15(E) sera. The other deletions could also be assigned to the smaller SFFV$_p$ genome based on measurements, and they appear to map in the region of the *pol* gene. Similar topographical features were observed by Bosselman et al. (3) in heteroduplexes of long cDNAs of F-MuLV and RNAs of SFFV, presumably of Friend virus polycythemia strain stocks.

(iii) Analysis of F-MuLV and SFFV$_a$ genomes. Heteroduplex analysis of F-MuLV and SFFV$_a$ (Fig. 4A to F) showed a more complex topography and further confirmed our results on the identification and location of the large *env* substitution seen in heteroduplexes of F-MuLV to F-MCF and SFFV$_p$. In spreads from 60% formamide, the large *env* substitution (Fig. 4C, segments e and f) was present and was of the same size as that seen in heteroduplexes with F-MCF and SFFV$_p$ and a minor substitution in the *gag* gene (Fig. 4C, segment m, features α and α′). This minor *gag* substitution showed complete homology in heteroduplexes between F-MCF and SFFV$_p$ under lower (40%) stringencies (Fig. 4F, segment m). Five major deletions were mapped. Three of these deletions occurred between the *env* and *gag* gene substitutions in the *pol* gene (Fig. 4C and F, segments h, j, and l). A deletion in p15(E) sequences (Fig. 4C and F, segment c), 3′ of the *env* gene substitution, was also discerned, as well as a deleted LTR (Fig. 4C and F, segment a) in the F-MuLV single-LTR clone. The position of this LTR deletion oriented the various deletion-substitution features, particularly when the lower stringency was used (Fig. 4D to F). With the 40% formamide conditions, the large *env* gene

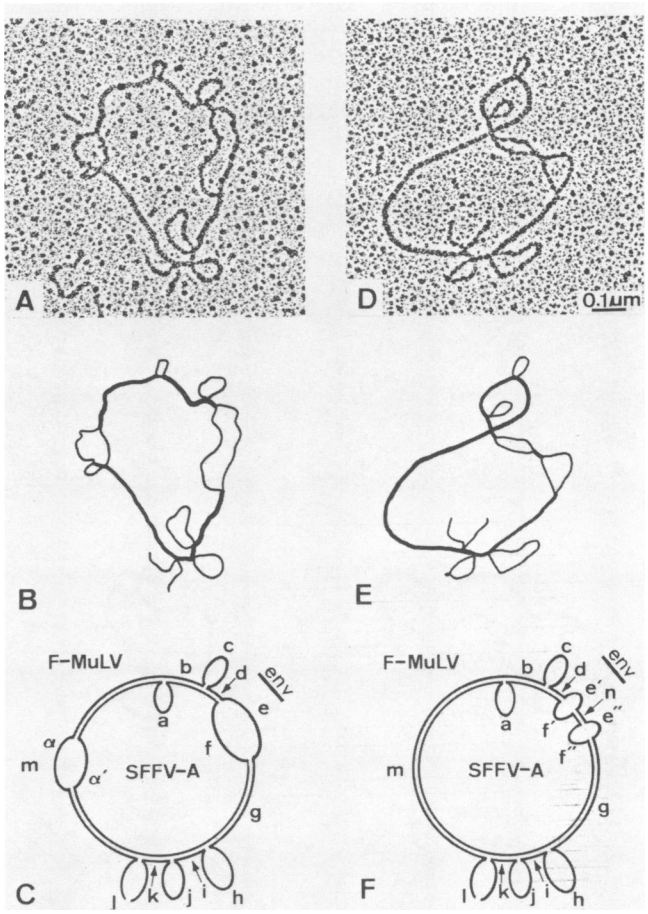

FIG. 4. Heteroduplex analysis of the relationship between F-MuLV and SFFV$_a$ clones. Heteroduplexes were mounted for electron microscopy from 60% (A to C) and 40% (D to F) formamide. (A and D) Actual heteroduplexes; (B and E) interpretive drawings; (C and F) schematic representations. The dimensions given in C and F are based on measurements of more than 20 molecules. Contour lengths (in kb) for C were as follows: a, 0.47 ± 0.05; b, 0.63 ± 0.14; c, 0.66 ± 0.09; d, 0.12 ± 0.02; e, 1.03 ± 0.09; f, 0.89 ± 0.09; g, 0.61 ± 0.09; h, 1.15 ± 0.07; i, 0.14 ± 0.02; j, 0.67 ± 0.07; k, 0.12 ± 0.02; l, 0.69 ± 0.03; m, 2.42 ± 0.13. The notations α and α′ mark an area of unpaired sequences which was seen in less than 30% of heteroduplexes and varied greatly in size. Dimensions for F-MuLV are b, c, d, e, g, h, i, j, k, l, and m; dimensions for SFFV$_a$ are a, b, d, f, g, i, k, and m. Contour lenghts (in kb) for F were as follows: a, 0.49 ± 0.08; b, 0.58 ± 0.05; c, 0.63 ± 0.05; d, 0.20 ± 0.06; e′, 0.39 ± 0.06; f′, 0.36 ± 0.03; n, 0.12 ± 0.04; e″, 0.41 ± 0.10; f″, 0.28 ± 0.09; g, 0.74 ± 0.09; h, 1.09 ± 0.09; i, 0.13 ± 0.02; j, 0.70 ± 0.06; k, 0.13 ± 0.01; l, 0.62 ± 0.04; and m, 2.55 ± 0.12. Dimensions for F-MuLV are b, c, d, e′, n, e″, g, h, i, j, k, l, and m; dimensions for SFFV$_a$ are a, b, d, f′, n, f″, g, i, k, and m.

substitution was reduced as in heteroduplexes of F-MuLV to F-MCF and $SFFV_p$, and it now demonstrated the common small region of homology in its middle (Fig. 4F, segment n).

(iv) Analysis of F-MCF and $SFFV_p$ genomes. The common size of substitutions in the same location of the *env* gene of F-MCF, $SFFV_p$, and $SFFV_a$; the immunological cross-reactivity of the gp52 of $SFFV_p$ and $SFFV_a$ with F-MCF gp70 (32, 35, 47); and the two-stage cotransfection data with 3′ subgenomic fragments (18, 22) suggest that this region contains some related and unique sequences responsible for the biological and pathogenic properties of these viruses. We therefore prepared heteroduplexes between F-MCF and $SFFV_p$ to examine this hypothesis. Figure 5A to F shows the results of this analysis. The only topographical features present at both high and low stringencies were three deletions in the $SFFV_p$ genome. One of these (Fig. 5C and F, segment f) was the same size as the p15(E) deletion demonstrated in heteroduplexes between F-MuLV and $SFFV_p$

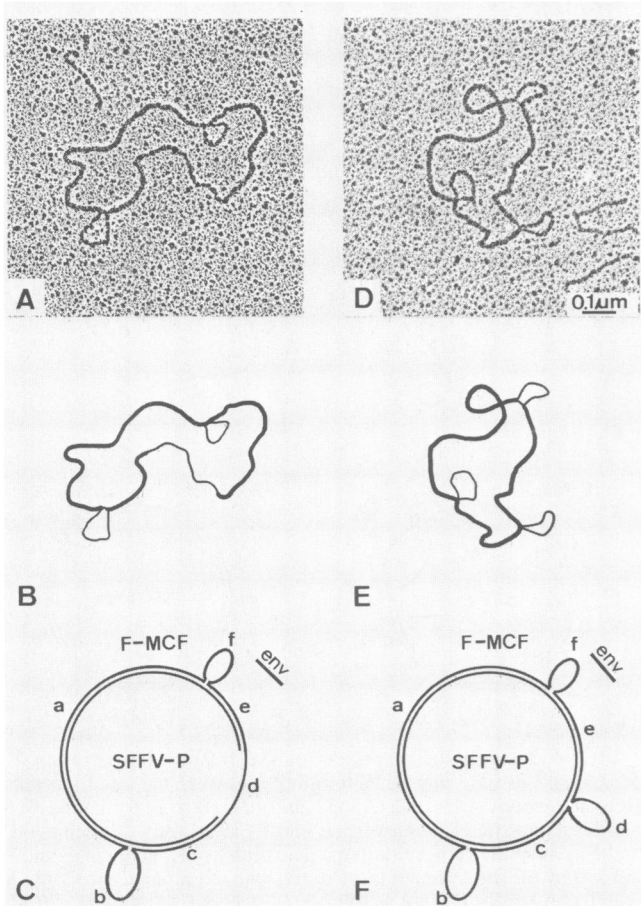

FIG. 5. Heteroduplex analysis of the relationship between F-MCF and $SFFV_p$ clones. Heteroduplexes were mounted for electron microscopy from 60% (A to C) and 40% (D to F) formamide. (A and D) Actual heteroduplexes; (B and E) interpretive drawings; (C and F) schematic representations. The dimensions given in panel C and F are based on measurements of over 20 molecules. Contour lengths (in kb) for C were as follows: a, 2.81 ± 0.11; b, 0.96 ± 0.09; c, 1.21 ± 0.07; d, 0.83 ± 0.06; e, 1.62 ± 0.06; and f, 0.71 ± 0.05. Dimensions for F-MCF are a, b, c, d, e, and f; dimensions for $SFFV_p$ are a, c, and e. Contour lengths (in kb) for F were as follows: a, 2.85 ± 0.11; b, 0.99 ± 0.08; c, 1.12 ± 0.06; d, 0.95 ± 0.08; e, 1.55 ± 0.12; and f, 0.72 ± 0.07. Dimensions for F-MCF are a, b, c, d, e, and f; dimensions for $SFFV_p$ are a, c, and e.

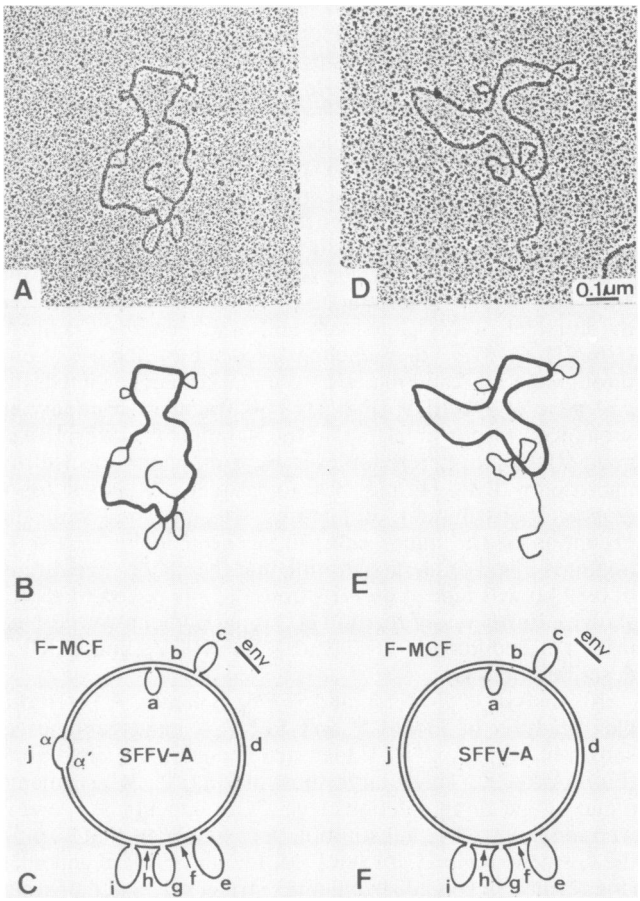

FIG. 6. Heteroduplex analysis of the relationship betwen F-MCF and $SFFV_a$ clones. Heteroduplexes were mounted for electron microscopy from 60% (A to C) and 40% (D to F) formamide. (A and D) Actual heteroduplexes; (B and E) interpretive drawings; (C and F) schematic representations. The dimensions given in panel C and F are based on measurements of more than 20 molecules. Contour lengths (in kb) for C were as follows: a, 0.59 ± 0.08; b, 0.80 ± 0.06; c, 0.62 ± 0.06; d, 1.54 ± 0.10; e, 0.97 ± 0.07; f, 0.13 ± 0.03; g, 0.73 ± 0.08; h, 0.12 ± 0.02; i, 0.81 ± 0.08; and j, 2.44 ± 0.30. The notations α and α′ mark an area of unpaired sequences, which was seen in less than 25% of the heteroduplexes and varied greatly in size. It is in a similar location to α and α′ in Fig. 4A to C. Dimensions for F-MCF are b, c, d, e, f, g, h, i, and j; dimensions for $SFFV_a$ are a, b, d, f, h, and j. Contour lengths (in kb) for F were as follows: a, 0.62 ± 0.08; b, 0.80 ± 0.07; c, 0.68 ± 0.06; d, 1.54 ± 0.05; e, 1.05 ± 0.05; f, 0.12 ± 0.02; g, 0.76 ± 0.08; h, 0.12 ± 0.02; i, 0.82 ± 0.09; and j, 2.33 ± 0.12. Dimensions for F-MCF are b, c, d, e, f, g, h, i, and j; dimensions for $SFFV_a$ are a, b, d, f, h, and j.

(Fig. 3) and $SFFV_a$ (Fig. 4). The other two deletions (Fig. 5C and F, segments b and d) were of the same size and location as *pol* gene deletions also mapped in heteroduplexes between F-MuLV and $SFFV_p$ (Fig. 3). Strikingly, the large *env* substitution was not seen in heteroduplexes between F-MCF and $SFFV_p$, even under the highest stringency tested (60% formamide), suggesting that their *env* genes, within the limits of resolution of heteroduplex technology, were very closely related, except for the deletion of p15(E) sequences from $SFFV_p$.

(v) Analysis of F-MCF and $SFFV_a$ genomes. Heteroduplexes of F-MCF and $SFFV_a$ clones were also analyzed. These heteroduplexes (Fig. 6A to F) showed the same complex topography of deletions and minor substitutions as

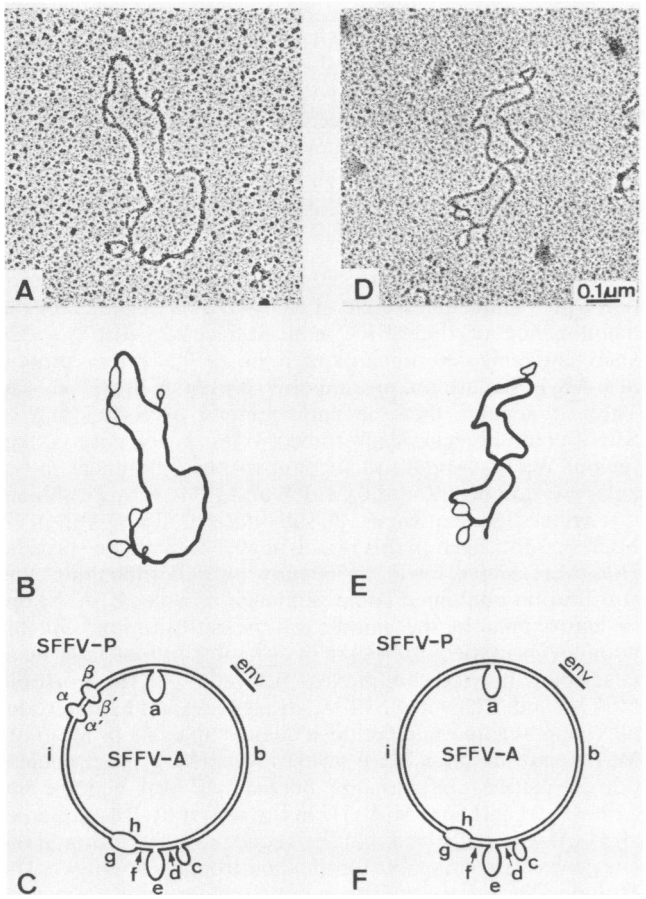

FIG. 7. Heteroduplex analysis of the relationship of SFFV$_p$ and SFFV$_a$ clones. Heteroduplexes were mounted for electron microscopy from 60% (A to C) and 40% (D to F) formamide. (A and D) Actual heteroduplexes; (B and E) interpretive drawings; (C and F) schematic representations. The dimensions given in C and F are based on measurements of over 20 molecules. Contour lengths (in kb) for C were as follows: a, 0.49 ± 0.05; b, 2.11 ± 0.12; c, 0.22 ± 0.02; d, 0.14 ± 0.03; e, 0.63 ± 0.06; f, 0.12 ± 0.02; g, 0.33 ± 0.03; h, 0.22 ± 0.02; and i, 2.33 ± 0.23. The notations α and α′ and β and β′ are minor substitutions that are present in less than 50% of measured heteroduplexes. They are located in the same region as the previously designated α and α′ in Fig. 4 and 6 (A to C). The dimensions for SFFV$_p$ are b, c, d, e, f, g, and i; dimensions for SFFV$_a$ are a, b, d, f, h, and i. Contour lengths (in kb) for F were as follows: a, 0.50 ± 0.07; b, 2.14 ± 0.13; c, 0.27 ± 0.04; d, 0.14 ± 0.02; e, 0.59 ± 0.08; f, 0.13 ± 0.02; g, 0.33 ± 0.06; h, 0.22 ± 0.03; and i, 2.17 ± 0.11.

that discerned in heteroduplexes of F-MuLV and SFFV$_a$ (Fig. 4) and again, strikingly, the *env* substitution was absent (Fig. 6C and F, segment d) between the *pol* and p15(E) deletions, suggesting that the glycoprotein coding regions were identical.

(vi) Analysis of SFFV$_p$ and SFFV$_a$ genomes. Since the heteroduplexes between the SFFVs and F-MCF did not reveal any significant differences that could account for the pathogenic properties of these viruses, we wanted to determine whether any minor differences in an additive relationship could be demonstrated in heteroduplexes between SFFV$_p$ and SFFV$_a$. That is, could we determine whether there was a greater divergence in the *env* sequences between SFFV$_p$ and SFFV$_a$ than between F-MCF and SFFV$_p$ or SFFV$_a$. Figure 7A to F shows the results of this examination. In spreads from 60% formamide, the presence of an additional LTR in SFFV$_a$ (Fig. 7C, segment a) and differences in amount and location of *pol* gene deletions and substitutions (Fig. 7C, segments c, e, g, and h) were readily apparent. Minor substitutions within the *gag* gene region (Fig. 7C, segment i, features α and α′, β and β′) were discerned in less than 50% of the molecules mapped. At lower formamide concentrations (40%), these substitutions were not present (Fig. 7F, segment i). These data further strengthened the earlier observation on the strong homology between the envelope coding regions of F-MCF, SFFV$_p$, and SFFV$_a$ genomes. It further defined the location of the p15(E) deletion as being exactly the same in both SFFV$_p$ and SFFV$_a$.

As a final examination of the *env* gene regions of these viruses, and to demonstrate the correctness of our bias for assignment of the minor substitutions (Fig. 7C, segment i, features α and α′, β and β′) at high stringency to the *gag* gene region and not the *env* gene, we performed heteroduplexing between the entire SFFV$_a$ genome and a complete 3′ *env* subgenomic SFFV$_p$ fragment. In addition to the *env* region of SFFV$_p$, this fragment, cut out of its vector by *Pst*I, contains a small *Pst*I to *Hin*dIII pBR322 sequence tail at the viral 5′ *Hin*dIII cloning site as a marker. This construct spread from 70% formamide clearly oriented the heteroduplex and demonstrated that no substitutions existed in the *env* region between SFFV$_p$ and SFFV$_a$ (data not shown).

Figure 8 is a schematic summary of the heteroduplex findings with unpermuted, colinear forms of the virus genomes.

DISCUSSION

Mammalian transforming retroviruses can be classified into two broad categories: those that have acquired rapid oncogenic potential through deletion of viral genes (*gag*, *pol*, or *env*) and recombination with one of a number of cellular oncogenes (15, 19), and those that are viral *env* gene recombinants (6, 8, 11, 17, 32). Viruses in the first category are capable of rapidly transforming cells in vivo or in vitro. In the latter category, only the SFFVs of the Friend virus complex act in an acute fashion; they are also replication defective, with their transforming activity being restricted to a specific erythroid precursor cell in vivo (12, 14, 25, 39, 43).

In this report, we have used detailed heteroduplex mapping studies to derive molecular information about the origin and distinctive biological properties of sequences responsible for the erythroproliferative diseases induced by SFFV$_p$ and SFFV$_a$. Heteroduplex mapping of SFFV$_p$ and SFFV$_a$ to replication-competent F-MuLV and F-MCF demonstrated that major deletions had occurred in the *pol* gene of each of the SFFVs, which would account for their replication defectiveness. For SFFV$_p$, two major deletions of 0.71 and 0.83 kbp were mapped in the *pol* gene, and a single deletion of 0.69 kbp was mapped in the p15(E) region of the *env* gene. Our results are in agreement with those of Clark and Mak (7), who have determined the complete nucleotide sequence of an infectious strain of SFFV$_p$; they demonstrated these three deletions and an additional large deletion of 0.15 kbp between the two *pol* gene deletions, and two minor, yet significant, deletions of 6 and 13 base pairs, respectively, in the *gag* gene. The size of the *gag* substitutions put them below the resolution of heteroduplex mapping; however, the finding of an additional deletion of 0.15 kbp by Clark and Mak (7) in their strain of SFFV$_p$ would have been resolved in our heteroduplexes had it been present. Its absence in our clone might represent SFFV$_p$ strain-specific differences between the clone used here and that of Clark and Mak.

Comparison of $SFFV_p$ with $SFFV_a$ further demonstrated that there were differences in the amount and location of these *pol* gene deletions and substitutions. The additional deletion that corresponds to the p15(E) coding sequences in F-MuLV and F-MCF was mapped to exactly the same site in the 3′ half of the *env* gene of $SFFV_p$ and $SFFV_a$; it also contributes to the overall defectiveness of these viruses. Minor substitutions were also observed in the *gag* gene of $SFFV_a$, only at high stringency (in 60% formamide spreads), and were not present in $SFFV_p$, F-MuLV, or F-MCF; this region in these genomes appeared identical under the same spreading conditions. Perhaps this difference can be accounted for by an additional recombinant event with a murine retrovirus unrelated to the replication-competent members of the Friend virus complex during passage of this strain over the years.

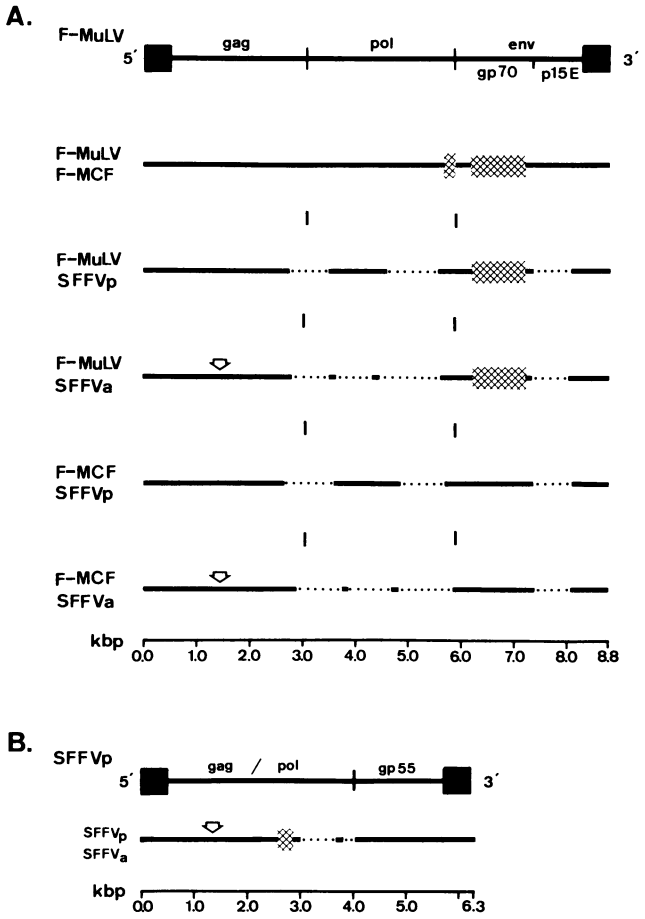

FIG. 8. Schematic summary of the heteroduplex findings from Fig. 2 to 7, using unpermuted colinear forms of the virus genomes. For this presentation, all genomes were considered to have two LTRs (one at the 5′ end and the other at the 3′ end of the heteroduplex molecule). (A) A complete double-stranded replication-competent F-MuLV genome (top) is shown indicating the relative positions of the *gag*, *pol*, *env*, and LTR (black boxes) regions. The gp70 and p15(E) coding sequences in *env* are indicated. All heteroduplex features are mapped relative to the replication-competent helper viruses (F-MuLV or F-MCF). In the F-MuLV and F-MCF heteroduplex, the features are mapped relative to F-MuLV. The thick solid line represents regions of homology. The hatched areas represent substitutions in the F-MCF or replication-defective $SFFV_p$ and $SFFV_a$ genomes relative to F-MuLV. The dotted lines indicate deleted sequences in the $SFFV_p$ and $SFFV_a$ genomes relative to the replication-competent F-MuLV or F-MCF. The open arrows indicate regions of minor substitutions in the *gag* gene detected in less than 50% of the molecules at high stringency. (B) A complete double-stranded replication-defective $SFFV_p$ genome (top) is shown indicating the relative positions of remaining *gag*, *pol*, and gp55 (*env*) sequences. The thick solid line represents regions of homology. The hatched areas represent substitutions between $SFFV_p$ and $SFFV_a$, and the dotted lines indicate deleted sequences in $SFFV_a$ relative to $SFFV_p$. The open arrow denotes regions of minor substitution found in less than 50% of the molecules.

$SFFV_p$ and $SFFV_a$-infected cells synthesize a glycoprotein with a molecular weight of 52,000 that is essential for the maintenance of the SFFV-induced disease; SFFV gp52s share antigenic determinants with the gp70 envelope protein of F-MCF that are not present on F-MuLV gp70 (32, 35, 47). Thus, it appears that the pathogenicity of each strain of SFFV could be genetically traced to the 3′ *env* gene coding region. We first sought to account for the differences in the antigenic composition of F-MuLV and F-MCF by examining the *env* coding sequences. A substitution of 0.89 kbp in F-MCF was localized in this region in 60% formamide spreads. However, under lower stringency (40% formamide), this substitution contained some sequence homology (0.12 kbp) in approximately the middle of the substitution. Similar homologies in the gp70 region of *env* substitutions have been described in heteroduplexes between AKR ecotropic MuLVs and MCFs and $SFFV_p$ viruses (29) and by heteroduplex mapping and nucleotide sequence analysis of Moloney MuLV and Moloney MCF viruses (4) and by direct nucleotide sequence comparisons between F-MuLV (20) and $SFFV_p$ by Clark and Mak (7). In the report by Bosselman et al. (4), it was suggested that the sequence substitution in the *env* gene was responsible for the dual-tropic properties of the Moloney MCF viruses. The major substitution that exists in the gp70 region of the *env* gene of F-MuLV and F-MCF probably also accounts for the differences in their host range specificities and pathogenicity (6, 30).

The most striking finding was in the heteroduplexes of SFFVs to F-MuLV and F-MCF, which showed a complete conservation of F-MCF gp70 sequences in both $SFFV_p$ and $SFFV_a$. Thus, one could hypothesize that both $SFFV_p$ and $SFFV_a$ are derived from F-MCF or possibly another closely related MCF species of *env* sequences; the results further suggested tha these sequences were identical in $SFFV_p$ and $SFFV_a$.

Since the heteroduplexes between the SFFVs and F-MCF did not reveal any significant differences in the *env* region that could account for the pathogenic properties of these viruses, we wanted to determine whether any minor differences in sequence divergence in an additive relationship could be demonstrated by comparing the molecular clones of $SFFV_p$ and $SFFV_a$. This analysis showed no differences in the envelope coding region, even under the most stringent (70% formamide) spreading conditions, thus strengthening the hypothesis on the relationship of F-MCF, $SFFV_p$, and $SFFV_a$. Furthermore, the heteroduplexes of the SFFVs to F-MCF showed unambiguously that no additional large substitutions, i.e., viral oncogenes (15, 19), are present in $SFFV_p$ or $SFFV_a$ that could account for the differences in their leukemogenicity.

The murine mink cell focus-inducing leukemia viruses are believed to arise by recombination between ecotropic MuLV and other *env* genes, perhaps those of xenotropic MuLVs (11, 34). Extensive restriction enzyme mapping of MCF genomes by Chattopadhyay et al. (6), oligonucleotide and peptide mapping studies by Green et al. (16), and the

discovery of distinct receptors for MCFs (30), collectively argue for the involvement of specific MCF genomes in the recombination event and not xenotropic MuLVs as originally proposed. The cytopathic MCFs are thymotropic and appear to play a role in the development of thymic leukemias in mice (6, 8). In contrast to the leukemogenicity and target cell specificities of *env* sequences in replication-competent MCFs, these sequences in the SFFVs cause disease only in erythroid cells. Recently, Chatis et al. (5) reported that when a 621-nucleotide-long fragment of the T-cell tropic Moloney MuLV, encompassing the U3 region of its LTR, was used to replace the corresponding region in the F-MuLV genome, the resulting recombinant virus induced almost exclusively T-cell lymphomas, instead of erythroleukemia. Their results suggest that both genetic elements, i.e., envelope glycoprotein and LTR, play a role in disease induction.

Based on our results, the apparent differences between $SFFV_p$ and $SFFV_a$ could only be accounted for by very minor changes in the genetic composition of these viruses. The nucleotide sequence analysis of the 3′ *env* sequences of $SFFV_p$ has shown that the presence of the large deletion spanning the junction of gp70 and p15(E) and two small insertions (of 1 and 6 bases, respectively) at the 3′ terminus of the gp52-encoding region, results in an $SFFV_p$ unique amino acid sequence (1, 7, 48). Thus, the $SFFV_p$ gp52 results from the fusion at its amino terminus of MCF-gp70 specific sequences and the remaining p15(E) sequences at its carboxy terminus. This may account for some of the unusual structural characteristics, aberrant processing, and pathogenic properties of the $SFFV_p$ and its gp52 coding sequences (1, 7, 48).

Differently processed envelope glycoproteins of similar structure may vary greatly in biological function. Such differences exist in the post-translational processing of $SFFV_p$ and $SFFV_a$ and correlate with the differences in the histology of the virus-induced disease (33). Our conclusions, based on the extensive heteroduplex mapping data presented here, are compatible with those derived from nucleotide sequencing of $SFFV_p$ and MCF *env* sequences (1, 4, 7, 48). One could predict that, based on the extensive homology demonstrated in heteroduplexes between $SFFV_p$ and $SFFV_a$, similar small molecular changes will be discovered upon nucleotide sequencing of $SFFV_a$, which will confer upon the $SFFV_a$ gp52 its unique biological and pathogenic properties.

ACKNOWLEDGMENTS

This work was supported in part by Public Health Service contract N01-CO-23910 with Program Resources, Inc., from the National Cancer Institute.

We are grateful for the skilled assistance of Joan Hopkins for typing this manuscript.

LITERATURE CITED

1. **Amanuma, H., A. Katori, M. Obata, N. Sagata, and Y. Ikawa.** 1983. Complete nucleotide sequence of the gene for the specific glycoprotein (gp55) of Friend spleen focus-forming virus. Proc. Natl. Acad. Sci. U.S.A. **80**:3913–3917.
2. **Axelrad, A. A., and R. A. Steeves.** 1964. Assay for Friend leukemia virus: rapid quantitation method based on enumeration of macroscopic spleen foci in mice. Virology **24**:513–518.
3. **Bosselman, R. A., L. J. L. D. Van Griensven, M. Vogt, and I. M. Verma.** 1980. Genome organization of retroviruses. IX. Analysis of the genomes of Friend spleen focus-forming (F-SFFV) and helper murine leukemia viruses by heteroduplex-formation. Virology **102**:234–239.
4. **Bosselman, R. A., F. van Straaten, C. Van Beveren, I. M. Verma, and M. Vogt.** 1982. Analysis of the *env* gene of a molecularly cloned and biologically active Moloney mink cell focus-forming proviral DNA. J. Virol. **44**:19–31.
5. **Chatis, P. A., C. A. Holland, J. W. Hartley, W. P. Rowe, and N. Hopkins.** 1983. Role for the 3′ end of the genome in determining disease specificity of Friend and Moloney murine leukemia viruses. Proc. Natl. Acad. Sci. U.S.A. **80**:4408–4411.
6. **Chattopadhyay, S. K., M. W. Cloyd, D. L. Linemeyer, M. R. Lander, E. Rands, and D. R. Lowy.** 1982. Cellular origin and role of mink cell focus-forming viruses in murine thymic lymphomas. Nature (London) **295**:25–31.
7. **Clark, S. P., and T. W. Mak.** 1983. Complete nucleotide sequence of an infectious clone of Friend spleen focus-forming provirus: gp55 is an envelope fusion glycoprotein. Proc. Natl. Acad. Sci. U.S.A. **80**:5037–5041.
8. **Cloyd, M. W., J. W. Hartley, and W. P. Rowe.** 1980. Lymphomagenicity of recombinant mink cells focus-inducing murine leukemia viruses. J. Exp. Med. **151**:542–552.
9. **Davis, R. W., and R. W. Hyman.** 1971. A study in evolution: the base sequence homology between coliphages T7 and T3. J. Mol. Biol. **62**:287–301.
10. **Davis, R. W., M. Simon, and N. Davidson.** 1971. Electron microscope heteroduplex methods for mapping regions of base sequence homology in nucleic acids. Methods Enzymol. **21**:413–428.
11. **Elder, J. H., J. W. Gautsch, F. C. Jensen, R. A. Lerner, J. W. Hartley, and W. P. Rowe.** 1977. Biochemical evidence that MCF murine leukemia viruses are envelope (*env*) gene recombinants. Proc. Natl. Acad. Sci. U.S.A. **74**:4676–4680.
12. **Frederickson, T., P. Tambourin, F. Wendling, C. Jasmin, and F. Smajda.** 1975. Target cell of the polycythemia-inducing Friend virus: studies with Myleran. J. Natl. Cancer Inst. **55**:443–446.
13. **Friend, C.** 1957. Cell-free transmission in adult swiss mice of a disease having the character of a leukemia. J. Exp. Med. **105**:307–318.
14. **Friend, C., M. C. Patuleia, and E. de Harven.** 1966. Erythrocytic maturation *in vitro* of murine (Friend) virus-induced leukemia cells. Natl. Cancer Inst. Monogr. **22**:505–522.
15. **Gilden, R. V., and H. Rabin.** 1982. Mechanisms of viral tumorgenesis. Adv. Virus Res. **27**:281–334.
16. **Green, N., H. Hiai, J. H. Elder, R. S. Schwartz, R. H. Khiroya, C. Y. Thomas, P. N. Tsichlis, and J. M. Coffin.** 1980. Expression of leukemogenic recombinant viruses asociated with a recessive gene in HRS/J mice. J. Exp. Med. **152**:249–264.
17. **Hartley, J. W., N. K. Wolford, L. J. Old, and W. P. Rowe.** 1977. A new class of murine leukemia virus associated with development of spontaneous lymphomas. Proc. Natl. Acad. Sci. U.S.A. **74**:789–792.
18. **Kaminchik, J., W. D. Hankins, S. K. Ruscetti, D. L. Linemeyer, and E. M. Scolnick.** 1982. Molecular cloning of biologically active proviral DNA of the anemia-inducing strain of spleen focus-forming virus. J. Virol. **44**:922–931.
19. **Klein, G.** 1982. Cell-derived oncogenes. Adv. Viral Oncol. **1**:3–262.
20. **Koch, W., G. Hunsmann, and R. Friedrich.** 1983. Nucleotide sequence of the envelope gene of Friend murine leukemia virus. J. Virol. **45**:1–9.
21. **Linemeyer, D. L., S. K. Ruscetti, J. G. Menke, and E. M. Scolnick.** 1980. Recovery of biologically active spleen focus-forming virus from molecularly cloned spleen focus-forming virus-pBR322 circular DNA by cotransfection with infectious type C retroviral DNA. J. Virol. **35**:710–721.
22. **Linemeyer, D. L., S. K. Ruscetti, E. M. Scolnick, L. H. Evans, and P. H. Duesberg.** 1981. Biological activity of the spleen focus-forming virus is encoded by a molecularly cloned subgenomic fragment of spleen focus-forming virus DNA. Proc. Natl. Acad. Sci. U.S.A. **78**:1401–1405.
23. **MacDonald, M. E., R. W. Mak, and A. Bernstein.** 1980. Erythroleukemia induction by replication-competent type C viruses cloned from the anemia- and polycythemia-inducing isolates of Friend leukemia virus. J. Exp. Med. **151**:1493–1503.
24. **Mirand, E. A., R. A. Steeves, L. Avila, and J. T. Grace, Jr.,** 1968. Spleen focus formation by polycythemic strains of Friend

leukemia virus. Proc. Soc. Exp. Biol. Med. **127**:900–904.
25. **Nasrallah, A. G., and M. P. McCarry.** 1976. Brief communication: *in vivo* distinction between a target cell for Friend virus (FVp) and murine hematopoietic stem cells. J. Natl. Cancer Inst. **57**:443–445.
26. **Oliff, A., G. L. Hager, E. H. Chang, E. M. Scolnick, H. W. Chan, and D. R. Lowy.** 1980. Transfection of molecularly cloned Friend murine leukemia virus DNA yields a highly leukemogenic helper-independent type C virus. J. Virol. **33**:475–486.
27. **Oliff, A., L. Collins, and C. Mirenda.** 1983. Molecular cloning of Friend mink cell focus-inducing virus: identification of mink cell focus-inducing virus-like messages in normal and transformed cells. J. Virol. **48**:542–546.
28. **Oliff, A., and S. Ruscetti.** 1983. A 2.4-kilobase-pair fragment of the Friend murine leukemia virus genome contains the sequences responsible for Friend murine leukemia virus-induced erythroleukemia. J. Virol. **46**:718–725.
29. **Rapp, U. R., E. Birkenmeier, T. I. Bonner, M. A. Gonda, and M. Gunnell.** 1983. Genome structure of mink cell focus-forming murine leukemia virus in epithelial mink lung cells transformed in vitro by iododeoxyuridine-induced C3H/MuLV cells. J. Virol. **45**:740–754.
30. **Rein, A.** 1982. Interference grouping of murine leukemia viruses: a distinct receptor for the MCF-recombinant viruses in mouse cells. Virology **120**:251–257.
31. **Ruscetti, S., L. Davis, J. Feild, and A. Oliff.** 1981. Friend murine leukemia virus-induced leukemia is associated with the formation of mink cell focus-inducing viruses and is blocked in mice expressing endogenous mink cell focus-inducing xenotropic viral envelope genes. J. Exp. Med. **154**:907–920.
32. **Ruscetti, S., D. Troxler, D. Linemeyer, and E. Scolnick.** 1980. Three laboratory strains of spleen focus-forming virus: comparison of their genomes and translational products. J. Virol. **33**:140–151.
33. **Ruscetti, S. K., J. A. Feild, and E. M. Scolnick.** 1982. Polycythaemia- and anemia-inducing strains of spleen focus-forming virus differ in post translational processing of envelope-related glycoproteins. Nature (London) **294**:663–665.
34. **Ruscetti, S. K., D. Linemeyer, J. Feild, D. Troxler, and E. M. Scolnick.** 1978. Type-specific radioimmunoassays for the gp70s of mink cell focus-inducing murine leukemia viruses: expression of a cross-reacting antigen in cells infected with the Friend strain of a spleen focus-forming virus. J. Exp. Med. **148**:654–663.
35. **Ruscetti, S. K., D. Linemeyer, J. Feild, D. Troxler, and E. M. Scolnick.** 1979. Characterization of a protein found in cells infected with the spleen focus-forming virus that shares immunological cross-reactivity with the gp70 found in mink cell focus-inducing virus particles. J. Virol. **30**:787–798.
36. **Schultz, A. M., S. K. Ruscetti, E. M. Scolnick, and S. Oroszlan.** 1980. The *env*-gene of the spleen focus-forming virus lacks expression of p15(E) determinants. Virology **107**:537–542.
37. **Steeves, R. A.** 1975. Spleen focus-forming virus in Friend and Rauscher leukemia virus preparations. J. Natl. Cancer Inst. **54**:289–297.
38. **Steeves, R. A., R. J. Eckner, M. Bennett, E. A. Mirand, and P. J. Trudel.** 1971. Isolation and characterization of a lymphatic leukemia virus in the Friend virus complex. J. Natl. Cancer Inst. **46**:1209–1217.
39. **Tambourin, P., and F. Wendling.** 1971. Malignant transformation and erythroid differentiation by polycythaemia-inducing Friend virus. Nature (London) New Biol. **234**:230–233.
40. **Troxler, D. H., J. K. Boyars, W. P. Parks, and E. M. Scolnick.** 1977. Friend strain of spleen focus-forming virus: a recombinant between mouse type C ecotropic viral sequences and sequences related to xenotropic virus. J. Virol. **22**:361–372.
41. **Troxler, D. H., D. Lowy, R. Howk, H. Young, and E. M. Scolnick.** 1977. Friend strain of spleen focus-forming virus is a recombinant between ecotropic murine type C virus and the *env* gene region of xenotropic type C virus. Proc. Natl. Acad. Sci. U.S.A. **74**:4671–4675.
42. **Troxler, D. H., W. P. Parks, W. C. Vass, and E. M. Scolnick.** 1977. Isolation of a fibroblast nonproducer cell line containing the Friend strain of the spleen focus-forming virus. Virology **76**:602–615.
43. **Troxler, D. H., S. K. Ruscetti, D. L. Linemeyer, and E. M. Scolnick.** 1980. Helper-independent and replication-defective erythroblastosis-inducing viruses contained within anemia-inducing Friend virus complex (FV-A). Virology **102**:28–45.
44. **Troxler, D. H., S. K. Ruscetti, and E. M. Scolnick.** 1980. The molecular biology of Friend virus. Biochim. Biophys. Acta **605**:305–324.
45. **Troxler, D. H., and E. M. Scolnick.** 1978. Rapid leukemia induced by cloned Friend strain of replicating murine type C virus: association with induction of xenotropic-related RNA sequences contained in spleen focus-forming virus. Virology **85**:17–27.
46. **Troxler, D. H., E. Yuan, D. Linemeyer, S. Ruscetti, and E. M. Scolnick.** 1978. Helper-independent mink cell focus-inducing strains of Friend murine type C virus: potential relationship to the origin of replication-defective spleen focus-forming virus. J. Exp. Med. **148**:639–653.
47. **Wolff, L., R. Koller, and S. Ruscetti.** 1982. Monoclonal antibody to spleen focus-forming virus-encoded gp52 provides a probe for the amino-terminal region of retroviral envelope proteins that confers dual tropism and xenotropism. J. Virol. **43**:472–481.
48. **Wolff, L., E. Scolnick, and S. Ruscetti.** 1983. Envelope gene of the Friend spleen focus-forming virus: deletion and insertions in 3′ gp70/p15E coding region have resulted in unique features in the primary structure of its protein product. Proc. Natl. Acad. Sci. U.S.A. **80**:4718–4722.
49. **Young, H. A., M. A. Gonda, D. DeFeo, R. W. Ellis, K. Nagashima, and E. M. Scolnick.** 1980. Heteroduplex analysis of cloned rat endogenous replication-defective (30S) retrovirus and Harvey murine sarcoma virus. Virology **107**:89–99.